

Modeling of pressure-induced charge transfer character in piezoluminescent pyridylvinylanthracene crystals: Supporting Information

Josianne Owona,^{abc} David Casanova,^{cd} Lionel Truflandier,^a Frédéric Castet,^{a*} and Claire Tonnelé^{cd*}

^aUniversity of Bordeaux, CNRS, Bordeaux INP, ISM, UMR 5255, F-33405 Talence, France

^bUniversidad del País Vasco/Euskal Herriko Unibertsitatea (UPV/EHU), PK 1072, 20080 Donostia, Euskadi, Spain

^cDonostia International Physics Center, 20018 Donostia, Euskadi, Spain

^dIKERBASQUE - Basque Foundation for Science, 48009 Bilbo, Euskadi, Spain

E-mails: frederic.castet@u-bordeaux.fr; claire.tonnele@dipc.org

Contents

1.	<i>Structural parameters of the crystal polymorphs</i>	2
2.	<i>Non-Covalent Interaction (NCI) plots</i>	4
3.	<i>Electronic structure of the crystal polymorphs</i>	5
4.	<i>Phonon Density of States of C2</i>	8
5.	<i>Structural and optical properties of BP2VA in the gas phase</i>	9
6.	<i>Structural properties of the BP2VA molecular units in the crystal environment</i>	10
7.	<i>BP2VA excited state relaxation and electron-vibration coupling</i>	11
8.	<i>Classical approximation of dipole-dipole interactions in BP2VA dimers</i>	12
9.	<i>Low-lying states of BP2VA dimers extracted from the different crystal polymorphs</i>	13
10.	<i>Diabatization of the low-lying excited states of BP2VA dimers in the S₀ geometry</i>	14
11.	<i>Emission properties of BP2VA dimers extracted from the different crystal polymorphs</i>	15
12.	<i>Diabatization of the low-lying excited states of BP2VA dimers in the S₁ geometry</i>	16
13.	<i>Structural and optical properties of BP2VA in THF</i>	18
14.	<i>Relative stability of the crystal polymorphs</i>	19
15.	<i>References</i>	19

1. Structural parameters of the crystal polymorphs

Table S1: Geometrical parameters including space group, formula unit (Z), volume (\AA^3) and lattice parameters (translation vectors a , b , c (\AA) and angles α , β , γ (degrees) of the unit cell of the three BP2VA crystals, from XRD, optimized with $P = 0$ GPa and applied pressure of $P = 7.92$ GPa. For $P = 0$ GPa, deviations (dev.) of the calculated parameters (%) are calculated with respect to the XRD parameters. For $P = 7.92$ GPa, deviations (dev.) of the calculated parameters (%) are calculated with respect to the optimized parameters at $P = 0$ GPa.

	Atoms	Space group	Volume per molecule	dev.	a	dev.	b	dev.	c	dev.	$\alpha = \gamma$	β	dev.
XRD	C1	$C2/c$	505.5	-	16.02	-	8.12	-	15.55	-	90	92	-
	C2	$P2_1/c$	501	-	5.74	-	7.59	-	23.01	-	90	91	-
	C3	$P2_1/c$	488	-	10.19	-	20.53	-	10.42	-	90	116	-
Calc.	C1	$C2/c$	483	-4%	15.63	-2%	8.02	-1%	15.43	-1%	90	91	-1%
	C2	$P2_1/c$	484.5	-3%	5.75	-2%	7.57	-1%	22.27	-3%	90	91	0%
	C3	$P2_1/c$	466	-5%	10.01	-2%	20.42	-0.5%	10.29	-1%	90	118	1%
$P = 79.2$ kbar	C1	$C2/c$	366.5	-24%	14.64	-6%	7.49	-7%	13.39	-13%	90	87	-4%
	C2	$P2_1/c$	368	-24%	5.19	-10%	7.22	-5%	19.70	-12%	90	95	4%
	C3	$P2_1/c$	362	-22%	8.52	-15%	20.29	-1%	9.54	-7%	90	119	1%
no imposed sym. $P = 79.2$ kbar	C1	$P1$	371	-23%	14.43	-8%	7.69	-4%	13.41	-13%	90	87	-4%
	C2	$P1$	366	-24%	4.95	-14%	7.34	-3%	20.24	-12%	90	96	5%
	C3	$P1$	362	-22%	8.52	-15%	20.29	-1%	9.53	-8%	90	119	2%

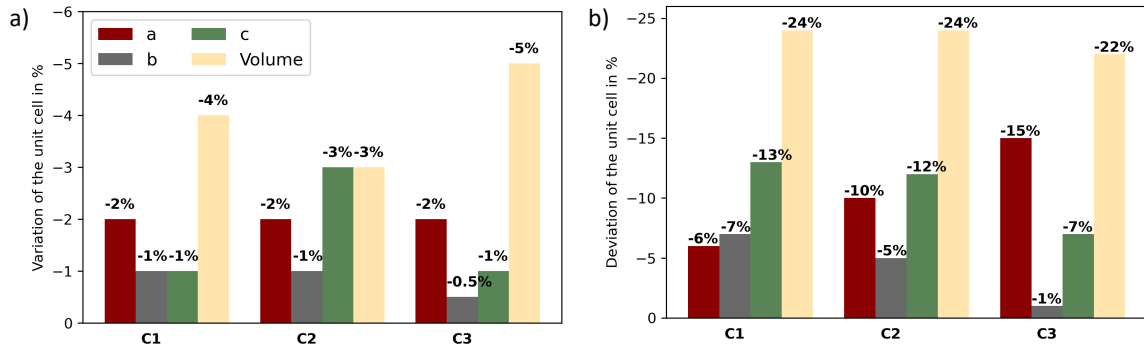


Figure S1: a) Variation of the unit cell volume (\AA^3) and of the translation vectors with respect to experimental data in three crystal polymorphs at $P = 0$ GPa. b) Change in the unit cell volume (\AA^3) and translation vectors in the three optimized crystals from zero pressure to $P = 7.92$ GPa.

Table S2. Intermolecular rotation parameters around the x, y and z molecular axes in experimental single crystals, and calculated under zero pressure and at 7.92 GPa.

		Twist	Tilt	Roll
C1	Exp	147	180	180
	P = 0	147	180	180
	P = 7.92	144	180	180
C2	Exp	133	180	180
	P = 0	133	180	180
	P = 7.92	129	180	180
C3	Exp	112	180	180
	P = 0	111	180	180
	P = 7.92	108	180	180

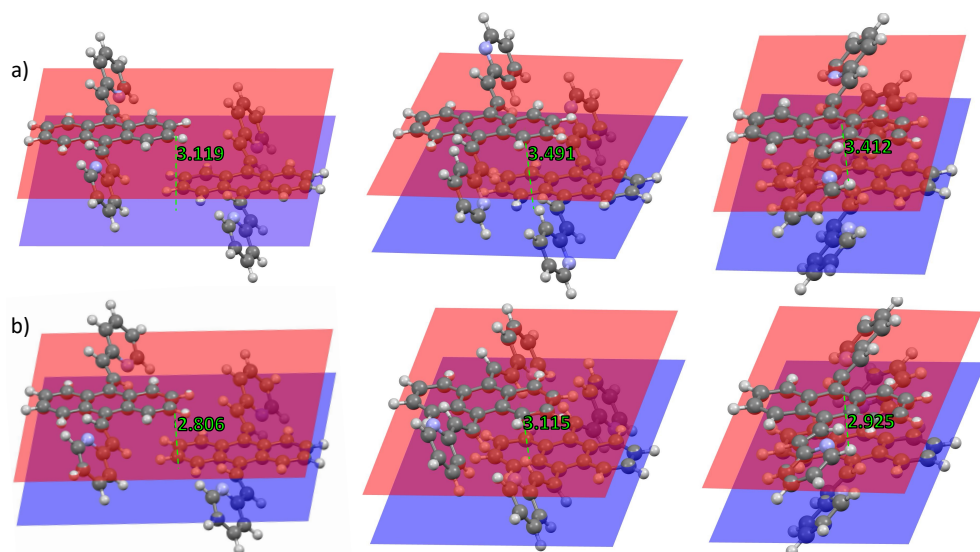
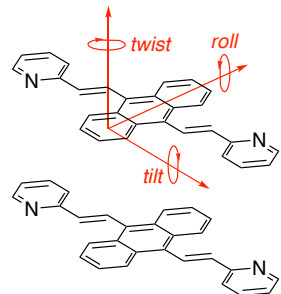


Figure S2: Dimeric structures extracted from the three optimized polymorphs (from left to right: C1, C2, C3) under a) $P = 0$ GPa (top) and b) $P = 7.92$ GPa (bottom). Intermolecular distances (\AA) between mean anthracene planes are reported (top from left to right: 3.119, 3.491, 3.412 \AA , bottom from left to right: 2.806, 3.115, 2.925 \AA).

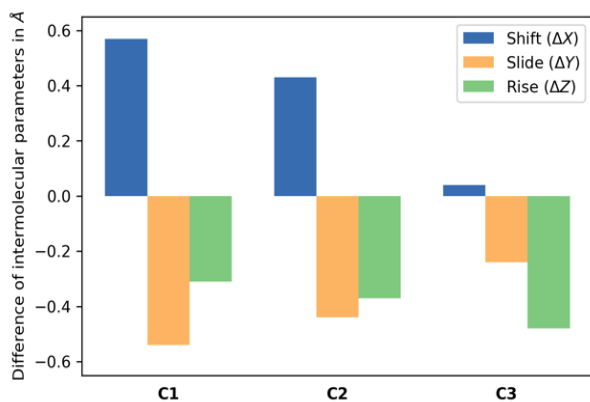


Figure S3: Differences in the intermolecular translation parameters between crystal polymorphs optimized at $P = 0$ GPa and at $P = 7.92$ GPa.

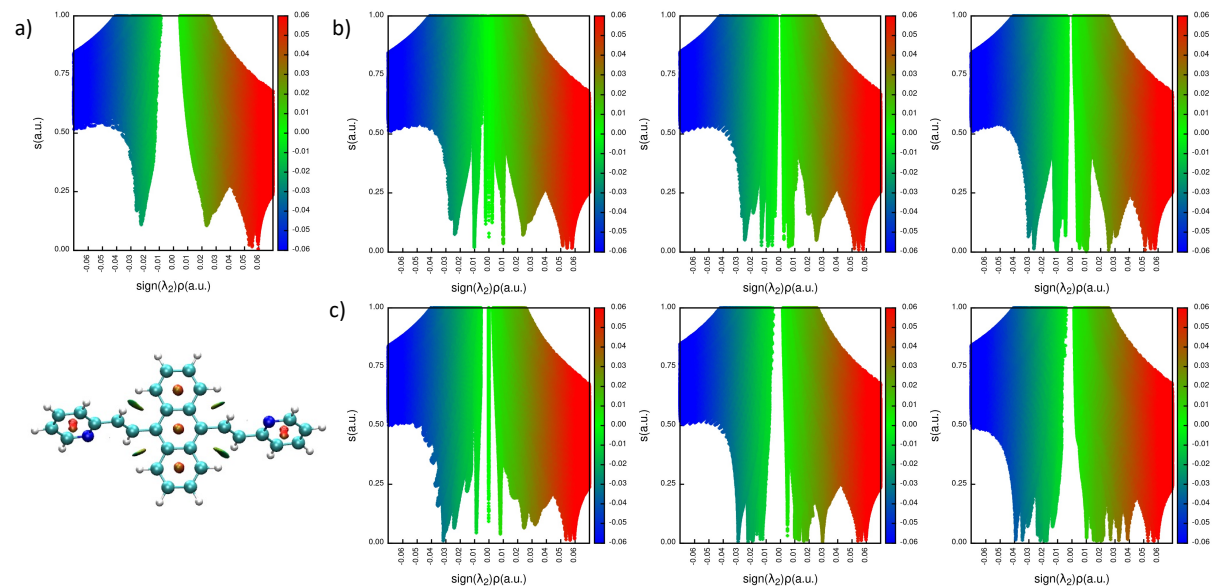
2. Non-Covalent Interaction (NCI) plots

In the NCI approach, weak intermolecular interactions appear if there is a drastic change in the reduced density gradient ($s(\rho)$) in the region located between the interacting atoms, resulting in density critical points between them. These points can be associated with troughs in the $s(\rho)$ plots, which, when visualized in real space, give rise to noncovalent interaction regions. The more troughs are present, the bigger is the NCI region.^{1,2} In addition to that, the strength and nature of the interaction can be evaluated by multiplying the sign of the second eigenvalue (λ_2) of the density Hessian matrix with the density ($sign(\lambda_2) \times \rho$). If $\lambda_2 < 0$, the region is characterised by attractive interactions and if $\lambda_2 > 0$, repulsive interactions can be observed. Van der Waals (vdW) interactions are observed for values of $sign(\lambda_2) \times \rho$ close to zero.

The noncovalent interactions in the monomer are shown in Figure S4a. Its NCI plot reveals that the interactions between the hydrogen atoms of the anthracene core and those of the methine bridges (green area) determine the equilibrium structure. It also reveals the presence of steric repulsion interaction within the five aromatic rings of the monomer (red area).

In Figure S4b, the NCI analysis reveals an overall increase in the number of troughs with $sign(\lambda_2) \times \rho$ close to zero (green areas) along the C1-C3 series. The presence of these troughs at low density is characteristic of an accumulation of weak vdW interactions, consistent with the increase in the number of intermolecular atomic contacts due to the higher overlap between monomers when moving from C1 to C3. Effects of pressure on the noncovalent interactions have been addressed in Figures 2b and S4c. Mainly, pressure moderately strengthens the interactions as indicated by the shift in the position of the troughs towards more negative values of $sign(\lambda_2) \times \rho$ (more attractive). Interestingly, the intramolecular hydrogen-hydrogen interactions in the monomers are also affected by pressure (shift of the blue troughs towards negative values in Figure S4c).

In summary, the analysis of the NCI plots suggests that the interaction between the monomers is dominated by weak vdW interactions. The applied pressure has a weak impact on the strength of the intermolecular interactions.



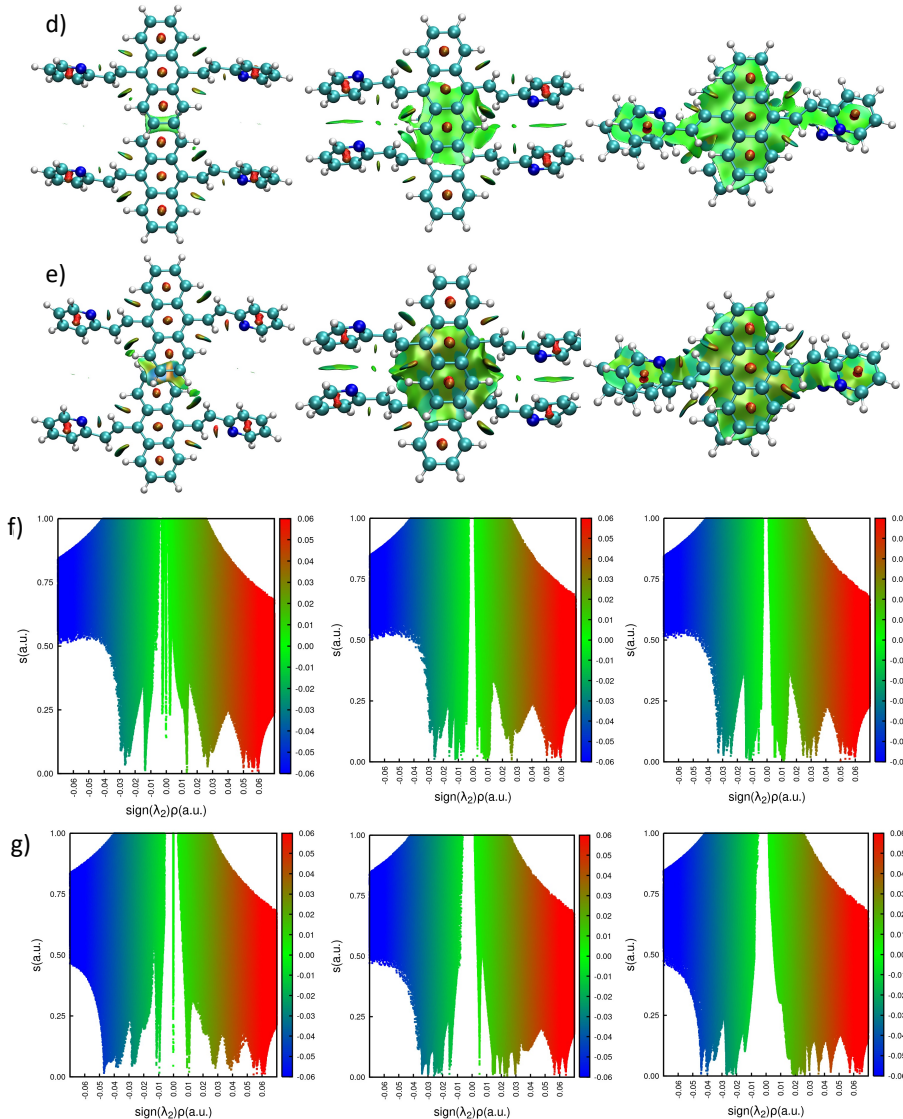


Figure S4: Reduced density gradient $s(\rho)$ vs $\text{sign}(\lambda_2) \times \rho$ plots of a) the monomer and dimers extracted from the three optimized polymorphs (from left to right: C1, C2, C3) optimized under b) $P = 0$ GPa and c) $P = 7.92$ GPa. Blue regions are associated with strong attractive interactions ($\lambda_2 < 0$), green regions are associated with weak van der Waals (vdW) interactions ($\lambda_2 \lesssim 0$) and red regions are associated with strong repulsive interactions ($\lambda_2 > 0$). Peaks that appear at $\rho \sim 0.01$ a.u. are for vdW interactions and $\rho \sim 0.05$ a.u. for hydrogen bonds. d, e) NCI plots and f, g) reduced density gradient plots of C1, C2, C3 at their relaxed S₁ geometry at ambient conditions and $P = 7.92$ GPa.

3. Electronic structure of the crystal polymorphs

$P = 0$ GPa

$P = 7.92$ GPa

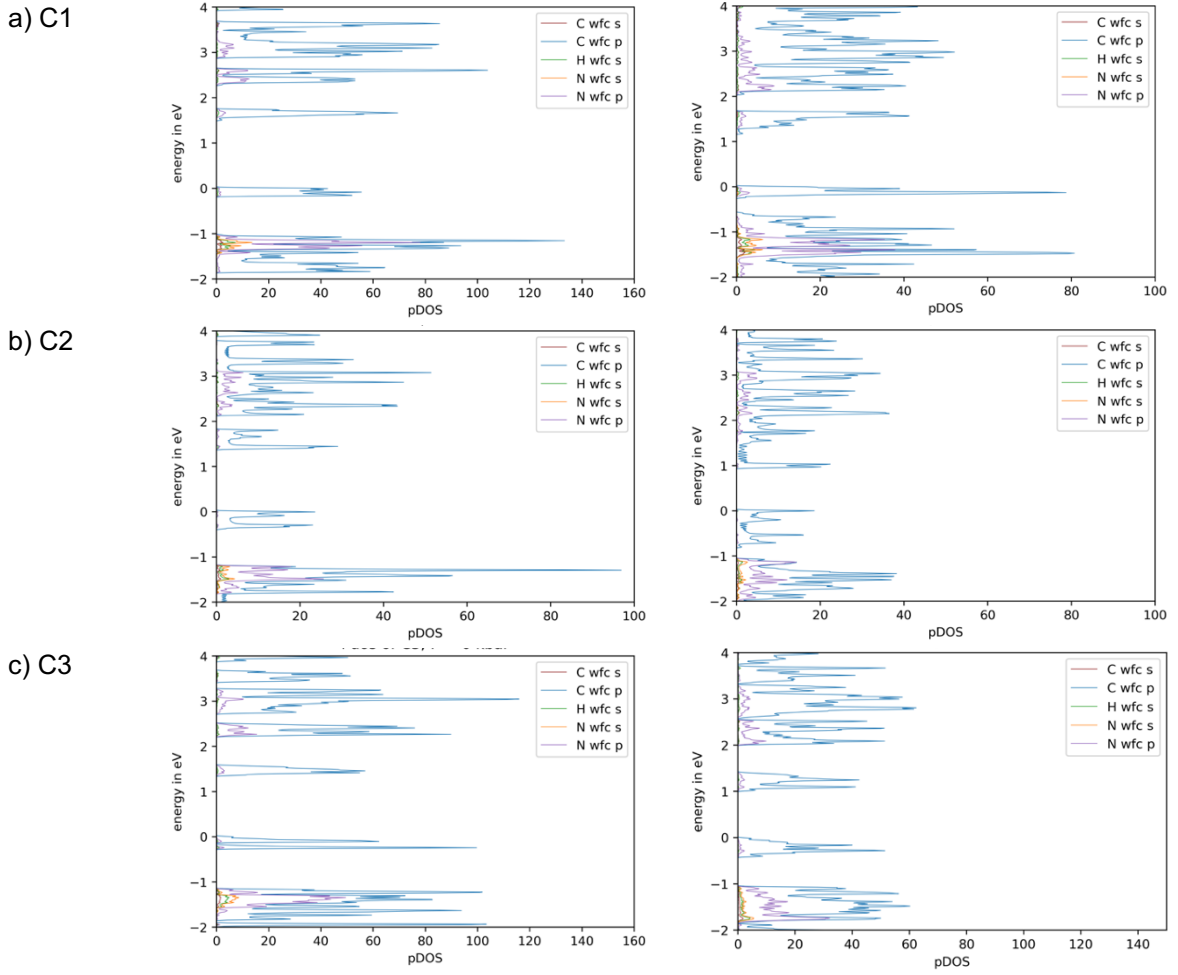


Figure S5: Projected densities of states of C1 (top), C2 (middle) and C3 (bottom) under $P = 0$ GPa and $P = 7.92$ GPa (right).

Table S3: Indirect and direct band gaps (eV) between the valence band maximum and the conduction band minimum for crystals C1, C2 and C3 at $P = 0$ GPa and $P = 7.92$ GPa.

	Indirect gap		Direct gap	
	$P = 0$ GPa	$P = 7.92$ GPa	$P = 0$ GPa	$P = 7.92$ GPa
C1	1.502	1.173	1.526	1.173
C2	1.386	0.946	1.441	1.011
C3	1.357	1.025	1.432	1.139

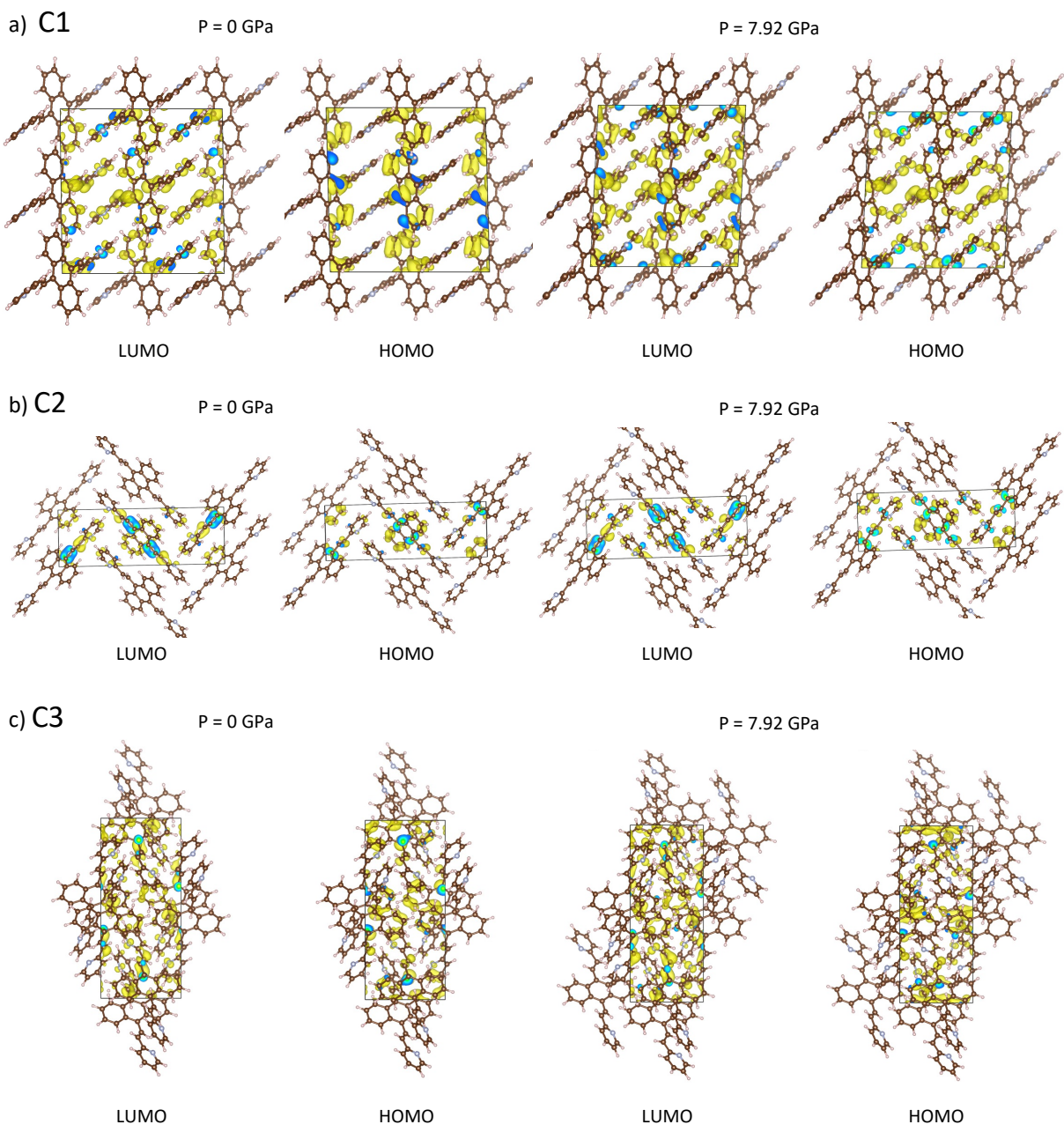


Figure S6: Highest occupied and lowest unoccupied crystalline orbitals at the Γ point of the first Brillouin zone, represented for the crystalline polymorphs C1, C2 and C3 at ambient and high pressures. Crystalline orbitals for C1, C2 and C3 are visualized with isosurface values of 0.0005, 0.001, 0.0006, respectively.

4. Phonon Density of States of C2

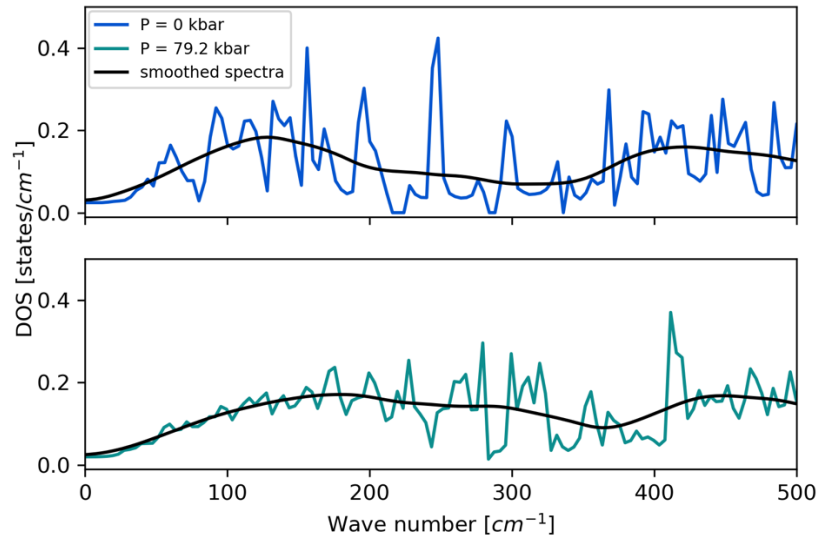
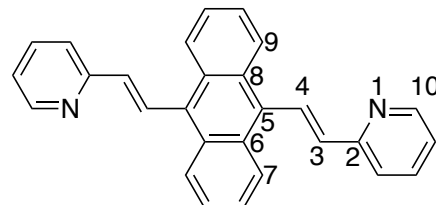


Figure S7: Phonon density of states (DOS) up to 500 cm⁻¹ of the C2 polymorph optimized at P = 0 GPa (blue) and P = 7.92 GPa (green).

5. Structural and optical properties of BP2VA in the gas phase

Table S4. Bond distances (\AA) and dihedral angles (degrees) of BP2VA in the equilibrium S_0 and S_1 geometries, optimized at the CAM-B3LYP/6-31G(d,p) level in gas phase.



Structural parameters	S_0	$S_1^{(a)}$	
C5-C4	1.477	1.439	1.423
C4-C3	1.336	1.357	1.366
C3-C2	1.471	1.456	1.448
C2-N1	1.341	1.347	1.350
N1-C10	1.328	1.326	1.325
θ C5-C4-C3-C2	178.6	179.4	-178.1
θ C8-C5-C4-C3	-124.5	-141.5	156.5
θ C6-C5-C4-C3 (θ_A)	56.6	35.1	-18.4
θ C7-C6-C5-C4	2.2	4.5	-25.8
θ C9-C8-C5-C4	2.0	6.0	20.3
θ C4-C3-C2-N1 (θ_B)	0.6	4.2	-4.8

(a) the two columns correspond to the two asymmetric molecular branches

Table S5: Vertical excitation energies to the low-lying excited states ($E_{S_0}^{vert}$, eV) and oscillator strengths ($f_{S_0}^{vert}$) calculated at the TDDFT/CAM-B3LYP/6-31G(d,p) and TDA/CAM-B3LYP/6-31G(d,p) levels using the geometry optimized at the CAM-B3LYP/6-31G(d,p) level in gas phase.

	TDDFT		TDA	
	$E_{S_0}^{vert}$	$f_{S_0}^{vert}$	$E_{S_0}^{vert}$	$f_{S_0}^{vert}$
S ₁	3.196	0.61	3.396	0.85
S ₂	4.012	0.00	4.068	0.00
S ₃	4.209	0.16	4.270	0.00
S ₄	4.219	0.00	4.283	0.07
S ₅	4.765	0.41	4.851	0.24
S ₆	4.792	0.00	4.861	0.00

6. Structural properties of the BP2VA molecular units in the crystal environment

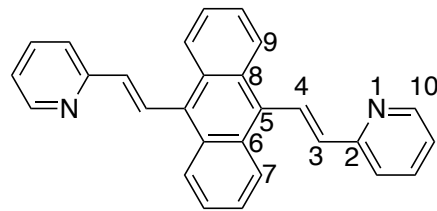


Table S6: Characteristic bond lengths (\AA) and dihedrals (degrees) of BP2VA extracted from the crystal polymorphs optimized with periodic DFT.

Structural parameters	C1		C2		C3			
	P=0	P=79.2	P=0	P=79.2	P=0^(a)		P=79.2^(a)	
C5-C4	1.463	1.439	1.467	1.450	1.460	1.461	1.434	1.435
C4-C3	1.351	1.347	1.350	1.342	1.353	1.354	1.348	1.351
C3-C2	1.462	1.451	1.461	1.441	1.463	1.460	1.441	1.444
C2-N1	1.354	1.346	1.356	1.344	1.356	1.354	1.348	1.347
N1-C10	1.335	1.326	1.338	1.324	1.336	1.332	1.323	1.329
θ C5-C4-C3-C2	177.3	172.3	179.1	178.1	-174.5	-179.7	178.1	177.4
θ C8-C5-C4-C3	-130.8	-132.9	-128.6	-129.3	142.4	-136.1	144.9	-167.4
θ C6-C5-C4-C3 (θ_A)	50.3	48.8	52.9	51.8	-39.5	45.6	-37.3	18.0
θ C7-C6-C5-C4	2.9	-0.4	-0.7	-5.9	-0.4	3.7	-1.4	-0.4
θ C9-C8-C5-C4	1.5	-1.2	3.7	0.8	-4.9	2.9	-4.6	8.0
θ C4-C3-C2-N1 (θ_B)	14.7	13.4	-167.5	-168.5	5.7	-1.7	-1.2	13.1

^(a)the two columns correspond to the two asymmetric molecular branches

Table S7: Characteristic bond lengths (\AA) and dihedrals (degrees) of the S₁ equilibrium geometry of BP2VA in a frozen crystal environment at ambient pressure, optimized using the ONIOM [CAM-B3LYP-D3/6-31G(d,p):UFF=QEQQ] level including electrostatic embedding.

Structural parameters	C1^(a)		C2^(a)		C3^(a)	
	P=0	P=79.2	P=0	P=79.2	P=0^(a)	P=79.2^(a)
C5-C4	1.433	1.435	1.444	1.443	1.433	1.434
C4-C3	1.357	1.356	1.353	1.353	1.360	1.356
C3-C2	1.453	1.452	1.454	1.454	1.448	1.451
C2-N1	1.347	1.348	1.346	1.346	1.347	1.347
N1-C10	1.324	1.325	1.326	1.327	1.324	1.327
θ C5-C4-C3-C2	-180	-179.3	179.6	-179.5	-176.6	-175.1
θ C8-C5-C4-C3	-141.4	139.8	-136.2	136.8	-147.3	149.0
θ C6-C5-C4-C3 (θ_A)	38.6	-39.8	45.9	-45.3	32.8	-31.1
θ C7-C6-C5-C4	6.9	-7.0	8.4	-8.3	10.0	-3.9
θ C9-C8-C5-C4	-0.04	-2.1	-1.3	1.1	0.9	-3.1
θ C4-C3-C2-N1 (θ_B)	14.6	-14.8	-163.4	162.7	2.4	1.9

^(a)the two columns correspond to the two asymmetric molecular branches

Table S8: Characteristic bond lengths (\AA) and dihedrals (degrees) of the S_1 equilibrium geometry of BP2VA in a frozen crystal environment at $P = 7.92 \text{ GPa}$, optimized using the ONIOM [CAM-B3LYP-D3/6-31G(d,p):UFF=QEQQ] level including electrostatic embedding.

Structural parameters	C1 ^(a)		C2 ^(a)		C3 ^(a)	
C5-C4	1.393	1.410	1.430	1.430	1.400	1.408
C4-C3	1.342	1.343	1.329	1.329	1.345	1.331
C3-C2	1.434	1.439	1.436	1.436	1.418	1.416
C2-N1	1.337	1.331	1.319	1.319	1.326	1.301
N1-C10	1.311	1.314	1.305	1.305	1.312	1.316
θ C5-C4-C3-C2	175.5	-173.5	-180.0	180.0	178.4	-177.7
θ C8-C5-C4-C3	-140.5	133.3	-126.6	126.6	147.1	167.0
θ C6-C5-C4-C3 (θ_A)	41.1	-43.0	56.6	-56.6	-38.3	-2.9
θ C7-C6-C5-C4	5.9	-3.0	4.8	-4.8	6.0	-2.5
θ C9-C8-C5-C4	-10.3	3.4	-11.8	11.8	-6.7	1.5
θ C4-C3-C2-N1 (θ_B)	14.0	-15.5	-174.8	174.8	-3.6	34.8

^(a)the two columns correspond to the two asymmetric molecular branches

7. BP2VA excited state relaxation and electron-vibration coupling

Normal mode analysis was performed with the FCclasses 3.1 code⁶ using the adiabatic Hessian potential energy surface model. Note that the large Huang-Rhys (HR) factors obtained for some normal modes suggest anharmonic behavior.

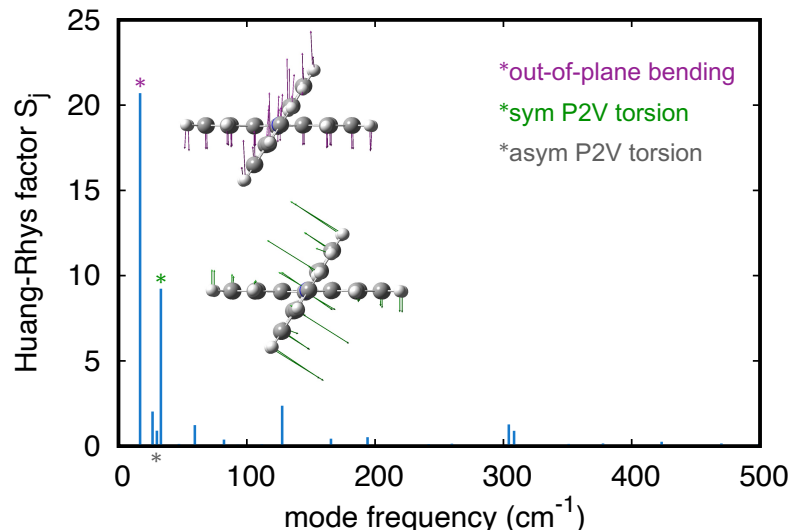


Figure S8. Huang–Rhys factor S_j of BP2VA normal modes as a function of the modes' frequency. Inset: normal modes associated with large HR factor: out-of-plane-bending mode (purple) and symmetric P2V torsion mode (green) at 17 and 33 cm^{-1} , respectively.

8. Classical approximation of dipole-dipole interactions in BP2VA dimers

The classical approximation of the dipole–dipole Coulomb interaction between transition dipoles of interacting monomers is expressed as:

$$V_{dd} = \frac{1}{4\pi\epsilon_0} \left[\frac{\mu_1 \cdot \mu_2}{|\mathbf{R}|^3} - 3 \frac{(\mathbf{R} \cdot \mu_1)(\mathbf{R} \cdot \mu_2)}{|\mathbf{R}|^5} \right]$$

where μ_1 and μ_2 are the transition dipole moments of each monomer and \mathbf{R} is the distance vector between the two transition dipoles. The gap between the lowest singlet states (Davydov splitting) is defined as: $\Delta E_{Dav} = 2V_{dd}$. The norm of the transition dipole moments calculated at the TDDFT/CAM-B3LYP/6-31G(d,p) level for the two interacting monomers in their crystal geometries at zero and under applied pressure is reported in Table S9, together with the intermolecular distance and the angle between the two transition dipole vectors. The Davydov splitting ΔE_{Dav} calculated at the TDDFT/CAM-B3LYP/6-31G(d,p) level and estimated using the point dipole approximation (PDA) are gathered in Table S10.

Table S9: Norm of the transition dipole moments (μ_1 and μ_2 , D) calculated at the TDDFT/CAM-B3LYP/6-31G(d,p) level for interacting monomers in their crystal geometries at ambient and under applied pressure, intermolecular distance \mathbf{R} (Å), angle (θ_{12} , degrees) between the two transition dipole vectors, and classical approximation of dipole-dipole interaction (V_{dd} , eV).

	P = 0 GPa			P = 7.92 GPa		
	C1	C2	C3	C1	C2	C3
μ_1	4.01	3.83	4.29	4.18	3.82	4.71
μ_2	4.01	3.83	4.30	4.18	3.82	4.72
\mathbf{R}	8.78	5.75	3.75	8.22	5.19	3.27
θ_{12}	0.07	179.81	179.98	0.01	0.25	179.94
V_{dd}	0.01	0.05	0.19	0.02	0.06	0.26

Table S10: Davydov splitting (eV) calculated at the TDDFT/CAM-B3LYP/6-31G(d,p) level and estimated using the point dipole approximation (PDA) as $\Delta E_{Dav} = 2V_{dd}$ for interacting monomers in their crystal geometries, at zero and under applied pressure. All values are in eV.

		C1	C2	C3
P = 0 GPa	TDDFT	0.05	0.06	0.20
	PDA	0.03	0.09	0.37
P = 7.92 GPa	TDDFT	0.07	0.14	0.19
	PDA	0.04	0.13	0.53

9. Low-lying states of BP2VA dimers extracted from the different crystal polymorphs

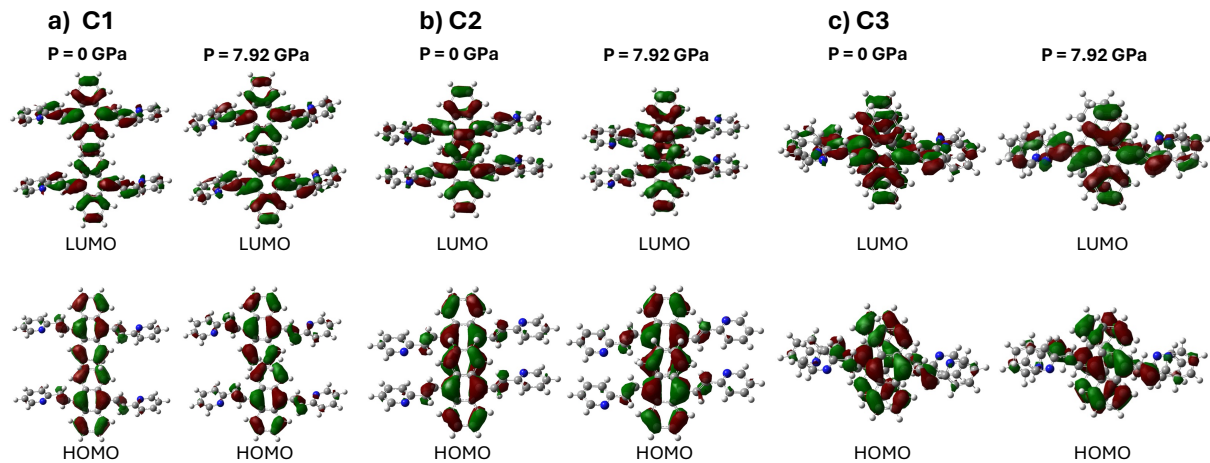


Figure S9: Shape of the frontier molecular orbitals of dimers in their S_0 geometry, as calculated by using the ONIOM approach at the [CAM-B3LYP-D3/6-31G(d,p):UFF=qeq]=embedcharge level for the three polymorphs.

Table S11: Vertical excitation energies (eV) and associated oscillator strengths, calculated for the closest molecular dimers extracted from the three crystal polymorphs at their respective ground state geometry, calculated at the TD and TDA/CAM-B3LYP/6-31G(d,p) level.

		$\Delta E (f) P = 0 \text{ GPa}$		$\Delta E (f) P = 7.92 \text{ GPa}$	
		TDDFT	TDADFT	TDDFT	TDADFT
C1	S_1	2.89 (0.00)	3.08 (0.00)	2.82 (0.00)	3.00 (0.00)
	S_2	2.94 (1.31)	3.15 (1.89)	2.89 (1.36)	3.09 (1.96)
	S_3	3.86 (0.01)	3.89 (0.00)	3.62 (0.00)	3.64 (0.00)
	S_4	3.86 (0.00)	3.90 (0.01)	3.69 (0.21)	3.71 (0.18)
C2	S_1	2.88 (0.00)	3.06 (0.00)	2.70 (0.58)	2.86 (0.74)
	S_2	2.95 (0.99)	3.15 (1.35)	2.84 (0.00)	3.01 (0.00)
	S_3	3.50 (0.00)	3.50 (0.00)	3.29 (0.00)	3.31 (0.00)
	S_4	3.55 (0.13)	3.56 (0.29)	3.59 (0.60)	3.64 (0.89)
C3	S_1	2.64 (0.00)	2.80 (0.00)	2.40 (0.00)	2.52 (0.00)
	S_2	2.84 (1.02)	2.97 (0.47)	2.59 (0.43)	2.65 (0.17)
	S_3	3.02 (0.00)	3.04 (0.00)	2.64 (0.00)	2.68 (0.00)
	S_4	3.05 (0.27)	3.16 (1.48)	2.77 (1.01)	2.99 (2.02)

10. Diabatization of the low-lying excited states of BP2VA dimers in the S₀ geometry

Table S12: Decomposition of the adiabatic states onto the diabatic basis for dimers (contributions in %) extracted from the crystal polymorphs in their ground state geometries at P = 0 GPa and P = 7.92 GPa. Calculations were performed at the TDA/CAM-B3LYP/6-31G(d,p) level. Constituting molecules of the dimers are labelled as A and B.

0 GPa		LE	CT	detailed contributions
C1	S ₁	99	/	51% LE _B + 48% LE _A
	S ₂	100	/	52% LE _A + 48% LE _B
	S ₃	/	99	59% CT _{AB} + 40% CT _{BA}
	S ₄	/	100	59% CT _{BA} + 41% CT _{AB}
C2	S ₁	99	2	50% LE _A + 49% LE _B + 1% CT _{AB} + 1% CT _{BA}
	S ₂	85	15	43% LE _B + 42% LE _A + 8% CT _{BA} + 7% CT _{AB}
	S ₃	2	99	50% CT _{BA} + 49% CT _{AB} + 1% LE _A + 1% LE _B
	S ₄	14	85	43% CT _{AB} + 42% CT _{BA} + 7% LE _A + 7% LE _B
C3	S ₁	87	12	44% LE _A + 43% LE _B + 6% CT _{AB} + 6% CT _{BA}
	S ₂	26	74	37% CT _{AB} + 37% CT _{BA} + 13% LE _A + 13% LE _B
	S ₃	12	87	44% CT _{BA} + 43% CT _{AB} + 6% LE _A + 6% LE _B
	S ₄	75	26	38% LE _B + 37% LE _A + 13% CT _{AB} + 13% CT _{BA}
7.92 GPa		LE	CT	detailed contributions
C1	S ₁	98	2	51% LE _A + 47% LE _B + 1% CT _{AB} + 1% CT _{BA}
	S ₂	100	/	52% LE _B + 48% LE _A
	S ₃	2	97	49% CT _{AB} + 48% CT _{BA} + 1% LE _A + 1% LE _B
	S ₄	/	100	51% CT _{BA} + 49% CT _{AB}
C2	S ₁	55	46	27% LE _A + 28% LE _B + 23% CT _{BA} + 23% CT _{AB}
	S ₂	91	9	46% LE _A + 45% LE _B + 5% CT _{AB} + 4% CT _{BA}
	S ₃	10	90	45% CT _{BA} + 45% CT _{AB} + 5% LE _A + 5% LE _B
	S ₄	46	54	27% CT _{BA} + 27% CT _{AB} + 23% LE _A + 23% LE _B
C3	S ₁	62	38	31% LE _A + 31% LE _B + 19% CT _{AB} + 19% CT _{BA}
	S ₂	8	92	46% CT _{AB} + 46% CT _{BA} + 4% LE _A + 4% LE _B
	S ₃	38	62	31% CT _{AB} + 31% CT _{BA} + 19% LE _A + 19% LE _B
	S ₄	92	8	46% LE _A + 46% LE _B + 4% CT _{AB} + 2% CT _{BA}

Table S13: Characterization of the diabatic states in terms of Mulliken charges of the two monomers A and B, and corresponding diabatic and adiabatic energies (in eV) calculated at the TDA/CAM-B3LYP/6-31G(d,p) level for dimers extracted from the crystal polymorphs in their ground state geometries at a) P = 0 GPa and b) P = 7.92 GPa.

a)	C1							b)	C1						
	Molecule A		Molecule B		Diabatic state		Molecule A		Molecule B		Diabatic state		Molecule A		Molecule B
Diabatic state	e^-	h^+	e^-	h^+	$E_{\text{adiabatic}}$	$E_{\text{adiabatic}}$	Diabatic state	e^-	h^+	e^-	h^+	$E_{\text{adiabatic}}$	$E_{\text{adiabatic}}$		
Z1	A^*B	-0.0021	0.0025	-0.9978	0.9972	3.12	3.08	Z1	A^*B	-0.9914	0.9904	-0.0085	0.0094	3.06	3.01
Z2	A^*B	-0.9977	0.9971	0.0021	0.0027	3.12	3.15	Z2	A^*B	-0.0087	0.0093	-0.9915	0.9906	3.06	3.09
Z3	A^+B^-	-0.1187	0.9443	-0.8808	0.0556	3.89	3.89	Z3	A^+B^-	-0.0838	0.8734	-0.9161	0.1264	3.67	3.64
Z4	A^-B^+	-0.8724	0.0544	-0.1270	0.9457	3.89	3.90	Z4	A^-B^+	-0.9179	0.1270	-0.0825	0.8725	3.67	3.71
C2															
Diabatic state	Molecule A		Molecule B		Diabatic state	e^-	h^+	e^-	h^+	$E_{\text{adiabatic}}$	$E_{\text{adiabatic}}$	Diabatic state	Molecule A		Molecule B
Diabatic state	e^-	h^+	e^-	h^+	Diabatic state	e^-	h^+	e^-	h^+	$E_{\text{adiabatic}}$	$E_{\text{adiabatic}}$	Diabatic state	e^-	h^+	$E_{\text{adiabatic}}$
Z1	A^*B	-0.9921	0.9921	-0.0078	0.0078	3.14	3.06	Z1	AB^*	-0.0208	0.0272	-0.9794	0.9729	3.12	2.87
Z2	AB^*	-0.0078	0.0078	-0.9922	0.9919	3.14	3.15	Z2	A^*B	-0.9795	0.9733	-0.0208	0.0272	3.13	3.01
Z3	A^-B^+	-0.9654	0.0097	-0.0347	0.9897	3.50	3.50	Z3	A^+B^-	-0.1153	0.9573	-0.8845	0.0426	3.29	3.31
Z4	A^+B^-	-0.0346	0.9899	-0.9657	0.0098	3.50	3.56	Z4	A^-B^+	-0.8847	0.0423	-0.1152	0.9574	3.29	3.64
C3															
Diabatic state	Molecule A		Molecule B		Diabatic state	e^-	h^+	e^-	h^+	$E_{\text{adiabatic}}$	$E_{\text{adiabatic}}$	Diabatic state	Molecule A		Molecule B
Diabatic state	e^-	h^+	e^-	h^+	Diabatic state	e^-	h^+	e^-	h^+	$E_{\text{adiabatic}}$	$E_{\text{adiabatic}}$	Diabatic state	e^-	h^+	$E_{\text{adiabatic}}$
Z1	A^*B	-0.9866	0.9818	-0.0127	0.0188	2.97	2.80	Z1	A^-B^+	-0.9464	0.0818	-0.0531	0.9182	2.65	2.52
Z2	AB^*	-0.0127	0.0187	-0.9868	0.9812	2.97	2.97	Z2	A^+B^-	-0.0535	0.9185	-0.9462	0.0815	2.65	2.65
Z3	A^-B^+	-0.9858	0.0287	-0.0139	0.9708	3.02	3.04	Z3	A^*B	-0.9549	0.9283	-0.0451	0.0717	2.77	2.68
Z4	A^+B^-	-0.0140	0.9709	-0.9860	0.0287	3.02	3.16	Z4	AB^*	-0.0454	0.0719	-0.9546	0.9283	2.77	2.99

Table S14: Diabatic Hamiltonian calculated at the TDA/CAM-B3LYP/6-31G(d,p) level for dimers extracted from the crystal polymorphs in their ground state geometries at P = 0 and P = 7.92 GPa. State energies and couplings are given in eV.

	0 GPa				7.92 GPa			
	LE _B	LE _A	CT _{AB}	CT _{BA}	LE _A	LE _B	CT _{AB}	CT _{BA}
	LE _B	3.12	-0.03	0.05	LE _A	3.06	0.04	-0.04
C1	LE _A	-0.03	3.12	0.03	LE _B	0.04	3.06	0.06
	CT _{AB}	0.05	0.03	3.89	CT _{AB}	-0.04	0.06	-0.04
	CT _{BA}	0.03	0.05	-0.01	CT _{BA}	0.06	-0.04	0.04
	LE _A	3.14	0.07	0.05	LE _B	3.12	-0.09	-0.15
C2	LE _B	0.07	3.14	0.10	LE _A	-0.09	3.13	0.24
	CT _{BA}	0.05	0.10	3.50	CT _{AB}	-0.15	0.24	3.29
	CT _{AB}	0.10	0.05	0.00	CT _{BA}	-0.24	0.15	0.00
	LE _A	2.97	-0.14	0.08	CT _{BA}	2.65	0.03	0.09
C3	LE _B	-0.14	2.97	0.00	CT _{AB}	0.03	2.65	0.01
	CT _{BA}	0.08	0.00	3.02	LE _A	0.09	0.01	2.77
	CT _{AB}	0.00	0.08	-0.01	LE _B	-0.01	-0.09	-0.19
	LE _A	2.97	0.08	3.02	LE _B	2.77	0.00	2.77

11. Emission properties of BP2VA dimers extracted from the different crystal polymorphs

Table S15. Intermolecular shifts^a along the three molecular axes (Δx , Δy and Δz , Å) and intramolecular torsion angles^a (θ_C and θ_D , degrees) in molecular dimers extracted from the three crystal polymorphs optimized at the ONIOM/CAM-B3LYP-D3/6-31G(d,p):UFF=qeq level including electrostatic embedding at their S₁ equilibrium geometries.

	P (GPa)	Shift (Δx)	Slide (Δy)	Rise (Δz)	θ_A^b	θ_B^b
C1	P = 0	-0.61	8.19	3.14	51/-51//40/-40	8/-8//14/-14
	P = 7.92	-1.12	7.54	2.94	47/-48//42/-43	14/-14//16/-15
C2	P = 0	0.32	-4.46	3.27	47/-45//61/-64	-165/163//175/177
	P = 7.92	-0.25	-4.03	2.95	60/-56//56/-60	180/175//175/-180
C3	P = 0	-1.27	1.17	3.30	48/-48//35/-30	-16/5//4/2
	P = 7.92	-0.78	0.76	2.81	-14/-39//39/14	41/0.4//0.4/-41

^a See Figure 1 for the definition of the structural parameters

^b molecule 1 right/left // molecule 2 right/left

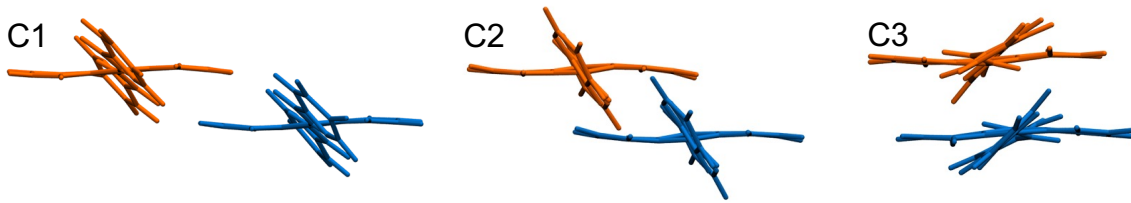


Figure S10. Relaxed S₁ geometry at high pressure for C1, C2 and C3 polymorphs.

Table S16: Vertical excitation energies (eV) and associated oscillator strengths calculated at the TD and TDA/CAM-B3LYP/6-31G(d,p) level for the closest molecular dimers at their respective S₁ geometry obtained at the ONIOM [CAM-B3LYP-D3/6-31G(d,p):UFF=qeq]=embedcharge level.

		ΔE (f) P = 0 GPa		ΔE (f) P = 7.92 GPa	
		TDDFT	TDADFT	TDDFT	TDADFT
C1	S ₁	2.48 (0.65)	2.72 (0.97)	2.52(0.60)	2.75 (0.85)
	S ₂	3.08 (0.70)	3.28 (1.04)	2.99 (0.74)	3.18 (1.10)
	S ₃	3.64 (0.01)	3.64 (0.01)	3.46 (0.07)	3.48 (0.08)
	S ₄	3.80 (0.04) ^a	3.79 (0.00)	3.56 (0.24)	3.58 (0.22)
C2	S ₁	2.48 (0.51)	2.72 (0.76)	2.38 (0.32)	2.56 (0.42)
	S ₂	3.06 (0.18)	3.16 (0.08)	2.78 (0.00)	2.96 (0.00)
	S ₃	3.32 (0.11)	3.39 (0.11)	3.13 (0.00)	3.17 (0.00)
	S ₄	3.50 (0.26)	3.57 (0.62)	3.60 (0.55) ^a	3.66 (0.76) ^a
C3	S ₁	2.36 (0.46)	2.58 (0.59)	2.27 (0.00)	2.37 (0.00)
	S ₂	2.78 (0.01)	2.79 (0.04)	2.65 (0.21)	2.71 (0.09)
	S ₃	2.97 (0.38)	3.02 (0.09)	2.87 (1.06)	2.97 (0.00)
	S ₄	3.09 (0.38)	3.26 (1.18)	2.89 (0.00)	3.11 (1.86)

^a adiabatic state S₅

12. Diabatization of the low-lying excited states of BP2VA dimers in the S₁ geometry

Table S17: Decomposition of the adiabatic states onto the diabatic basis for dimers (contributions in %) for the dimers at their relaxed excited state geometries at P = 0 GPa and P = 7.92 GPa. Calculations were performed at the TDA/CAM-B3LYP/6-31G(d,p) level. Constituting molecules of the dimer are labelled as A and B.

0 GPa		LE	CT	detailed contributions
C1	S ₁	99	/	99% LE _A
	S ₂	99	/	99% LE _B
	S ₃	/	99	99% CT _{BA}
	S ₄	/	99	99% CT _{AB}
C2	S ₁	95	5	95% LE _B + 3% CT _{BA} + 2% CT _{AB}
	S ₂	27	73	72% CT _{AB} + 26% LE _A + 1% LE _B + 1% CT _{BA}
	S ₃	28	72	55% CT _{BA} + 28% LE _A + 17% CT _{AB}
	S ₄	49	50	45% LE _A + 41% CT _{BA} + 9% CT _{AB} + 4% LE _B
C3	S ₁	93	6	88% LE _A + 6% CT _{BA} + 5% LE _B
	S ₂	7	93	93% CT _{BA} + 6% LE _A + 1% LE _B
	S ₃	6	94	94% CT _{AB} + 5% LE _B + 1% LE _A
	S ₄	93	6	88% LE _B + 6% CT _{AB} + 5% LE _A
7.92 GPa	LE	CT	detailed contributions	
C1	S ₁	98	1	97% LE _B + 1% LE _A + 1% CT _{BA}
	S ₂	94	5	93% LE _A + 4% CT _{AB} + 1% LE _B + 1% CT _{BA}
	S ₃	6	94	79% CT _{AB} + 15% CT _{BA} + 6% LE _A
	S ₄	1	99	83% CT _{BA} + 16% CT _{AB} + 1% LE _B
C2	S ₁	42	58	29% CT _{BA} + 29% CT _{AB} + 21% LE _A + 21% LE _B
	S ₂	68	32	34% LE _A + 34% LE _B + 16% CT _{BA} + 16% CT _{AB}
	S ₃	32	68	34% CT _{BA} + 34% CT _{AB} + 16% LE _A + 16% LE _B
	S ₄	58	42	29% LE _A + 29% LE _B + 21% CT _{BA} + 21% CT _{AB}
C3	S ₁	50	50	25% LE _A + 25% LE _B + 25% CT _{AB} + 25% CT _{BA}
	S ₂	4	96	48% CT _{AB} + 48% CT _{BA} + 2% LE _A + 2% LE _B
	S ₃	50	50	25% LE _A + 25% LE _B + 25% CT _{AB} + 25% CT _{BA}
	S ₄	96	4	48% LE _A + 48% LE _B + 2% CT _{AB} + 2% CT _{BA}

Table S18: Diabatic Hamiltonian calculated at the TDA/CAM-B3LYP/6-31G(d,p) level for dimers at their relaxed excited state geometries at P = 0 and P = 7.92 GPa. State energies and couplings are given in eV.

0 GPa					7.92 GPa			
C1	LE _A	LE _B	CT _{BA}	CT _{AB}	LE _B	LE _A	CT _{AB}	CT _{BA}
	2.73	-0.03	0.05	0.06	2.77	0.04	0.03	-0.08
	LE _B	3.28	0.04	0.03	LE _A	0.04	3.19	-0.07
	CT _{BA}	0.05	0.04	3.63	-0.01	CT _{AB}	0.03	-0.07
	CT _{AB}	0.06	0.03	-0.01	3.79	CT _{BA}	-0.08	0.04
C2	LE _B	CT _{AB}	LE _A	CT _{BA}	CT _{BA}	CT _{AB}	LE _A	LE _B
	2.76	-0.08	0.08	-0.14	3.07	-0.04	0.22	0.32
	CT _{AB}	-0.07	3.23	-0.13	0.00	CT _{AB}	-0.04	3.07
	LE _A	0.08	-0.13	3.41	-0.08	LE _A	0.22	0.32
	CT _{BA}	-0.14	0.00	-0.08	3.44	LE _B	0.32	0.08
C3	LE _A	CT _{BA}	CT _{AB}	LE _B	CT _{AB}	CT _{BA}	LE _B	LE _A
	2.63	0.05	0.00	0.15	2.69	0.03	-0.19	-0.11
	CT _{BA}	0.05	2.78	0.00	0.00	CT _{BA}	0.03	2.70
	CT _{AB}	0.00	0.00	3.03	0.06	LE _B	-0.19	0.11
	LE _B	0.15	0.00	0.06	3.21	LE _A	-0.11	0.19

13. Structural and optical properties of BP2VA in THF

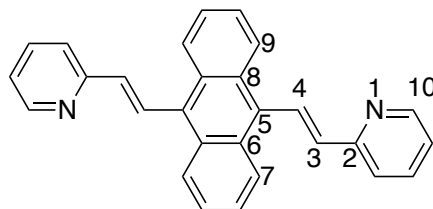
Table S19 reports the Franck-Condon vertical excitation energies ($E_{S_0}^{vert}$) and de-excitation energies from the S1 state minima ($E_{S_1}^{vert}$) for the BP2VA molecule in THF, using S_0 and S_1 geometries optimized at the CAM-B3LYP/6-31G(d,p) level. In addition to vertical transition energies, adiabatic energies, defined as the energy difference of the S_1 and S_0 states in their respective minimum ($E_{adia} = E_{S_1}^{opt} - E_{S_0}^{opt}$) were also evaluated, as well as the 0–0 energies, defined as the sum of the adiabatic contribution and the difference of zero-point vibrational energy (ZPVE) between S_1 and S_0 ($E_{0-0} = E_{adia} + \Delta E_{ZPVE}$), and which can be related to experimental crossing points between the absorption and fluorescence curves. Solvent effects were taken into account by using different implicit models. For both absorption and emission processes, we used i) the (non-equilibrium) integral equation formalism of the polarizable continuum model (IEF-PCM), as well as ii) the (non-equilibrium, state specific) external iteration (EI) procedure.^{3,4} In the standard IEF-PCM approach, the reaction field is defined using the ground state electron density. The EI approach employs a state-specific solvent reaction field that keeps the slow component (i.e. orientational changes of the solvent molecules) in equilibrium with the density of the originating state (S_0 for absorption and S_1 for emission), but allows the fast component (i.e. the electronic changes of the solvent molecules) to respond to the change in the solute's electron density.

Results reported in Table S19 show that the vertical absorption wavelength computed with IEF-PCM is in very good agreement with the experimental maximal absorption energy (3.07 vs 2.99 eV), while the EI approach describes better the experimental emission energy (2.19 vs 2.13 eV). The Stokes shift calculated using these two theoretical values is equal to 0.88 eV, in quantitative agreement with the experimental one (0.86 eV). The computed E_{0-0} energy (2.49 eV) is also in very good agreement with the crossing points between the absorption and fluorescence curves, estimated at ~2.6 eV from Ref [5].

Table S19: Vertical excitation energies ($E_{S_0}^{vert}$) and de-excitation energies from the S1 state minima ($E_{S_1}^{vert}$), as well as adiabatic and 0–0 energies computed at the CAM-B3LYP/6-31G(d,p) level for the BP2VA molecule in THF. Experimental data are taken from Ref [5]. All values are in eV.

	IEF-PCM	IEF-PCM (SS-EI)
$E_{S_0}^{vert}$	3.072	3.201
$E_{S_1}^{vert}$	1.957	2.193
E_{adia}	2.526	-
E_{0-0}	2.485	-
Stokes shift	1.115	1.008
Exp. absorption energy	2.988	
Exp. emission energy	2.127	
Exp. Stokes shift	0.861	
Exp. E_{0-0}		~2.6

Table S20. Bond distances (\AA) and dihedral angles (θ , degrees) of BP2VA in the equilibrium S0 and S1 geometries, optimized at the IEFPCM CAM-B3LYP/6-31G(d,p) level in tetrahydrofuran.



Atoms	S₀	S₁ ^(a)	
C5-C4	1.478	1.433	1.413
C4-C3	1.336	1.361	1.375
C3-C2	1.472	1.454	1.442
C2-N1	1.342	1.349	1.354
N1-C10	1.330	1.328	1.326
θ C5-C4-C3-C2	178.8	-179.993	-178.3
θ C8-C5-C4-C3	-124.7	-143.6	160.6
θ C6-C5-C4-C3 (θ _A)	56.5	33.2	-14.1
θ C7-C6-C5-C4	2.1	2.3	-28.1
θ C9-C8-C5-C4	2.1	8.5	23.2
θ C4-C3-C2-N1 (θ _B)	1.4	5.5	-4.6

^(a) the two columns correspond to the two asymmetric molecular branches

14. Relative stability of the crystal polymorphs

Table S21: Relative stability of the three optimized polymorphs at ambient and high pressure conditions (meV/atom).

	C1	C2	C3
P = 0 GPa	1.0	2.3	0.0
P = 7.92 GPa	21.4	24.1	0.0

15. References

- 1 E. R. Johnson, S. Keinan, P. Mori-Sánchez, J. Contreras-García, A. J. Cohen and W. Yang, *J. Am. Chem. Soc.* 2010, **132**, 6498–6506.
- 2 J. Contreras-García, E. R. Johnson, S. Keinan, R. Chaudret, J.-P. Piquemal, D. N. Beratan and W. Yang, *J. Chem. Theory. Comput.* 2011, **7**, 625–632.
- 3 R. Improta, V. Barone, G. Scalmani and M. J. Frisch, *J. Chem. Phys.* 2006, **125**, 054103.
- 4 R. Improta, G. Scalmani, M. J. Frisch and V. Barone, *J. Chem. Phys.* 2007, **127**, 074504.
- 5 Y. Dong, B. Xu, J. Zhang, X. Tan, L. Wang, J. Chen, H. Lv, S. Wen, B. Li, L. Ye, B. Zou and W. Tian, *Angew. Chem. Int. Ed.* 2012, **51**, 10782–10785.
- 6 J. Cerezo and F. Santoro, *J. Comput. Chem.* 2022, **44**, 626–643.